

# An Archaeobacterial Topoisomerase Homolog Not Present in Other Eukaryotes Is Indispensable for Cell Proliferation of Plants

Frank Hartung,<sup>1</sup> Karel J. Angelis,<sup>2</sup> Armin Meister,<sup>1</sup>  
Ingo Schubert,<sup>1</sup> Michael Melzer,<sup>1</sup>  
and Holger Puchta<sup>1,3</sup>

<sup>1</sup>Institute of Plant Genetics and  
Crop Plant Research (IPK)  
Corrensstrasse 3  
06466 Gatersleben  
Germany

<sup>2</sup>Institute of Experimental Botany  
CAS  
160 00 Prague 6  
Czech Republic

## Summary

Plants, in contrast to other eukaryotes, possess not only homologs of subunit A (AtSPO11-1, 2, 3) but also of subunit B (AtTOP6B) of the archaeobacterial topoisomerase VI [1]. AtTOP6B and AtSPO11-3 are strongly expressed in somatic tissue of *Arabidopsis* and are able to interact with each other *in vitro*. A T-DNA insertion in AtTOP6B results in deficient cell proliferation; plants stop growing at the rosette stage, have small crinkled leaves, and die about 4 weeks after germination. Cultured root cells die after a limited number of cell divisions. The mitotic index of the root meristems is strongly reduced. Flow cytometric analysis demonstrates that endoreplication in mutant plants is stopped at the 8C stage; the last cycle is not completed in most cases. Mutant plants show a significant increase in nuclear DNA strand breaks. A T-DNA insertion mutant of AtSPO11-3 has a phenotype that is almost to that of AtTOP6B and the double mutant. Thus, both genes seem to act *in vivo* as subunits of a functional entity. A loss of this function most likely results in a defect in DNA replication, leading directly, or via the activation of a DNA damage checkpoint, to an arrest of cell division and endoreduplication. The dependence on an archaeobacterial topoisomerase VI homolog distinguishes plants from the other eukaryotic kingdoms.

## Results and Discussion

DNA topoisomerases are enzymes that are required to change the topology of DNA molecules in basic processes like transcription and DNA replication in pro- and eukaryotes. In general, two classes of topoisomerases exist that can be discriminated by the kind of break they induce during their action on DNA molecules. Whereas class I topoisomerases induce a transient break in only one DNA strand, class II topoisomerase action is linked to a transient double-strand break [2, 3]. Surprisingly, archaeobacteria contain a unique subclass of type II topoisomerases, TopVI, which consists of subunits A and

B [4–6]. In eukaryotes, the homolog of subunit A, Spo11, is involved in inducing double-strand breaks (DSBs) during meiosis [7–11]. In contrast to other eukaryotes, plants contain three different homologs (SPO11-1, 11-2, 11-3) in their genome [1, 12]. The AtSpo11-1 homolog is involved in meiotic recombination, which is a role that is identical to that of Spo11 in other eukaryotes [13]. In addition, only plants contain a homolog of subunit B (TOP6B). Using two-hybrid analysis, we were able to show before that AtTop6B can interact with AtSpo11-2 and AtSpo11-3, but not with AtSpo11-1. Because AtTOP6B as well as AtSPO11-3 are strongly expressed in somatic tissue, we speculated that both proteins form a functional entity with an important role during vegetative growth of plants [1].

Screening the T-DNA insertion libraries of the *Arabidopsis* knockout facility in Madison, Wisconsin [14], we found a mutant of AtTOP6B. Segregation analysis, DNA blotting, and PCR analysis revealed a single insertion with two T-DNAs in inverse orientation (Figure 1A). The insertion is located in exon 12 and deleted 268 bp of the gene. Via RT-PCR, we were not able to detect any expression of the sequences behind the insertion site, indicating that, if any, only the first 397 of 670 amino acids of the AtTop6B protein could be expressed. Among the selfed progeny of the heterozygous mutant line, one quarter of the seedlings showed strong growth retardation. Using PCR, we could demonstrate that these plants were homozygous for the insertion. Heterozygous plants were phenotypically indistinguishable from wild-type. Homozygous plants developed small cotyledons and not more than two size-reduced leaf pairs per rosette (Figure 1B). Leaves turned yellowish, and plants died after 4–5 weeks. Transformation of plants heterozygous for the mutant with a 7.2-kb genomic clone carrying the AtTOP6B gene yielded the wild-type phenotype in the progeny homozygous for the mutant allele.

Electron microscopical studies of mutant seedlings 7 and 14 days after germination revealed morphological changes in the cytoplasm of the cotyledons. Whereas only few protein bodies were detected in wild-type, large agglomerations of protein bodies, peroxisomes, and small vacuoles were found in mutant plants (Figure 1C). In cells of 14-day-old mutant cotyledons, degradation of chloroplasts and all other cell organelles occurred.

To test whether the mutant is deficient in a specific developmental process or in cell proliferation in general, we explanted roots from mutant and wild-type plants soon after germination on MS plates complemented with plant hormones to induce callus culture [15]. Callus induction was less efficient for the mutant than for wild-type, and mutant calli grew slower (Figure 1D). Three weeks after induction, the mutant calli stopped growing and started to die. Thus, deficiency of AtTop6B results in a general growth defect. To test whether there is a deficiency in cell division, mitotic indices of root meristems of wild-type and mutant seedlings were deter-

<sup>3</sup>Correspondence: holger.puchta@bio.uka.de

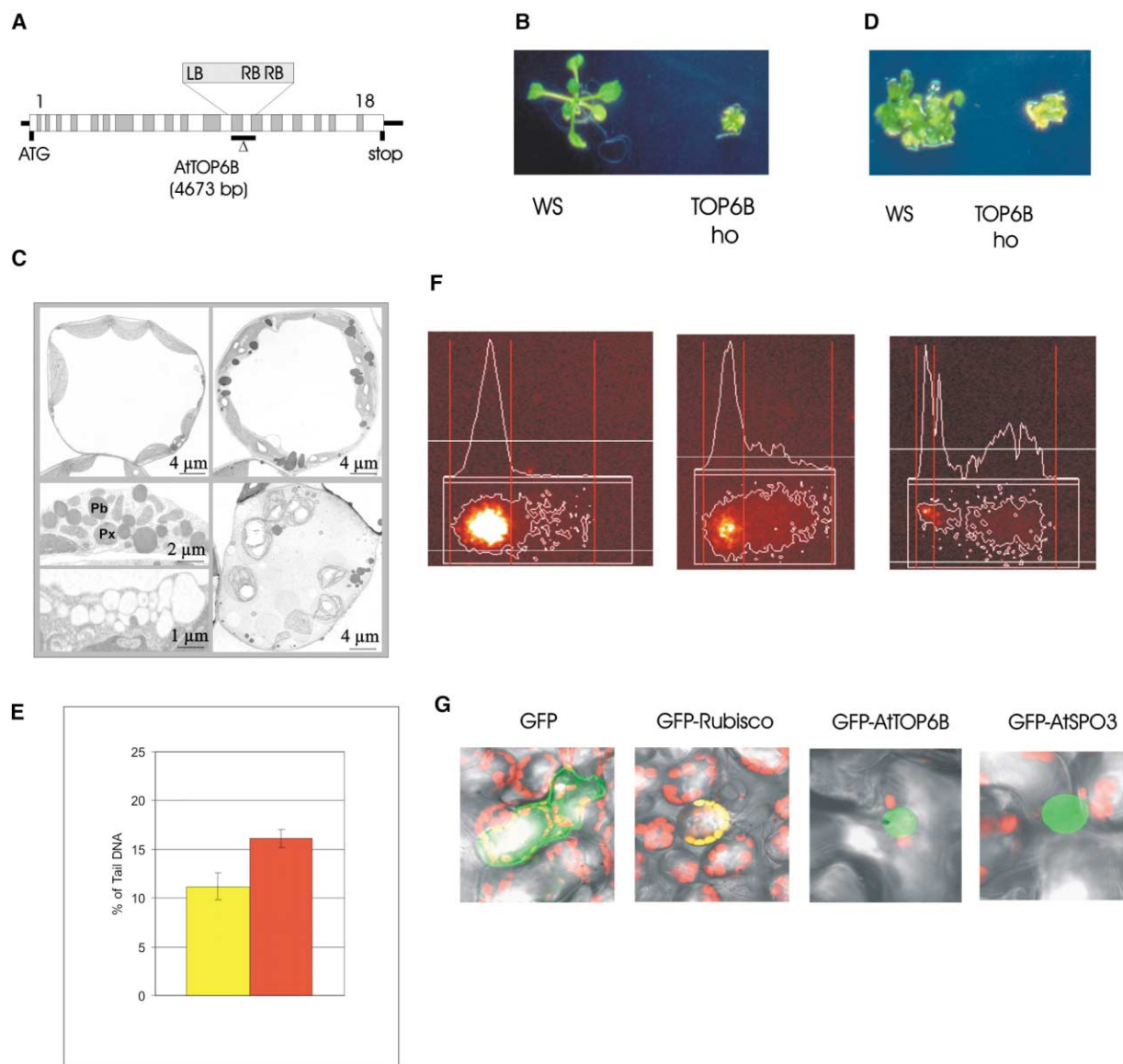


Figure 1. Characterization of the AtTOP6B Insertion Mutant of *Arabidopsis* WS

(A) Location of the T-DNA insertion within the gene. The T-DNA insertion is located in exon 12 and is combined with a deletion of 268 bp consisting of intron 12, exon 13, and part of intron 13. The insertion consists of two T-DNAs in an inverted orientation with a truncated left border (LB) at its 3' end.

(B) Comparison of a wild-type plant (left) and a plant homozygous for the T-DNA insertion in the AtTOP6B gene (right) 2 weeks after germination. (C) Electron microscopic analysis of cotyledons of the *Arabidopsis* mutant AtTOP6B. Spongy parenchyma cells of normal (top left) and dwarf (top right) growing seedlings. Details of the cytoplasm of the dwarf seedling with significant agglomerations of peroxisomes and protein bodies and an increasing number of small vacuoles (bottom left, Pb, protein body; Px, peroxisome). Spongy parenchyma of a 14-day-old dwarf growing seedling with symptoms of cell degeneration (bottom right).

(D) Induction of callus culture from roots of wild-type (left) and AtTOP6B-deficient plants (right) 4 weeks after the transfer of the roots to the callus-inducing medium.

(E) Statistical analysis of a comet assay. The average values of the percentage of DNA in tails of nuclei of 7-day-old seedlings of the AtTOP6B mutant (red) versus wild-type nuclei WS (yellow). Error bars indicate the standard error values. The medians of 200 comets on 8 individual gels represent 1 experimental point.

(F) A sample of comets from *Arabidopsis thaliana* nuclei. Left: a wild-type comet with only 10% DNA in the tail. Middle: a mutant nucleus with increased (30%) DNA in the tail. Such comets are typical representatives of DNA damage in mutant seedlings. Right: a severely fragmented mutant nucleus with 70% DNA in the tail. Such comets are rare, but they are more frequent in mutant than in wild-type nuclei. Apparently, the presence of less DNA is due to inefficient DNA staining of small fragments. This is the typical situation when cells undergo apoptosis.

(G) Identification of the cellular compartment to which AtTop6B and AtSpo11-3 are targeted (from left to right, GFP control, GFP fused to a chloroplastic-targeting signal, GFP fused to the N-terminal 144 aa of AtTop6B, GFP fused to the N-terminal 136 aa of AtSpo11-3). The red dots represent chloroplasts, the green dots represent GFP, and the yellow dots represent the GFP in chloroplasts (merged image). Both GFP fusions to the N termini of the topoisomerase homologs are targeted to the nucleus.

Table 1. Comparison of the Mitotic Indices within Root Meristems of *Arabidopsis* WS Wild-Type and the AtTOP6B Insertion Mutant

Wild-Type	top6B	Relation	$\chi^2$	p
30/970	6/994	5.1	16.29	0.0005
30/970	8/992	3.8	12.97	0.0005
38/962	16/984	2.4	9.21	0.005

The mitotic index is defined as the number of meta-, ana- and telophases/number of cells. A highly significant difference was found in all three independent experiments.

mined. The index of the mutant was between 2.5 and 5 times lower than that of wild-type (Table 1).

Type II topoisomerases are involved in decatenation of replication intermediates and in chromosome segregation [2, 3]. We speculated that unprocessed replication intermediates might be resolved unspecifically by tensional stress or nucleases, and we used the comet assay [16] to test whether nuclei of the mutant contained more DNA breaks. The amount of DNA in the comet tail separated from the nucleus is correlated with the number of breaks within the nuclear DNA. Indeed, significantly more breaks accumulate in the mutant (Figure 1E). Apoptotic nuclei, which occurred more frequently in the mutant, were not included in the statistical analysis (Figure 1F). We are tempted to speculate that, due to the accumulation of DNA damage, a cell cycle checkpoint is activated, resulting in a block of cell division and later in cell death. Multiple homologs of genes involved in DNA damage checkpoints have indeed been identified in the *Arabidopsis* genome [17, 18]; however, no mutants are available yet. DNA replication is also the basis of endoreduplication, a process of utmost importance for plant development [19, 20]. Using flow cytometry, we therefore tested the possible role of AtTOP6B in endoreduplication and indeed could show that, in contrast to wild-type plants, endoreduplication is stopped at the 8C level in the homozygous mutant (Figures 2A and 2B). Moreover, the 8C peak is shifted to a lower DNA content in the mutant, and this shift indicates that this endoreduplication cycle is not completed in at least most cells of

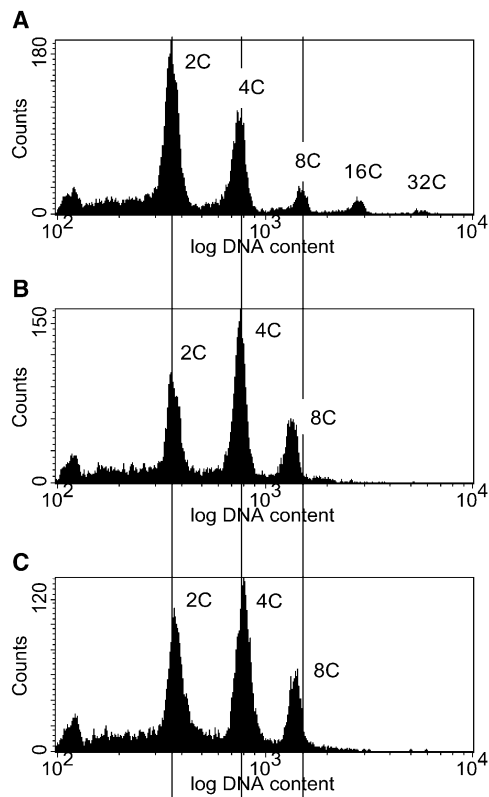


Figure 2. Flow Cytometric DNA Histogram of Nuclei from *Arabidopsis thaliana* Seedlings 2 Weeks after Germination

Comparison of DNA contents demonstrates that, in contrast to the 2C and 4C peak, the 8C peak is shifted to a lower DNA content in both mutants (vertical lines), and the 16C and 32C peaks are totally absent.

- (A) Wild-type.
- (B) The homozygous AtTOP6B mutant.
- (C) The homozygous AtSPO11-3 mutant.

the mutant (Figure 2B). Three (16C) and four (32C) endoreduplication cycles could be detected (Figure 2A) only in the wild-type seedlings.

Our results suggest that the nuclear DNA is the target

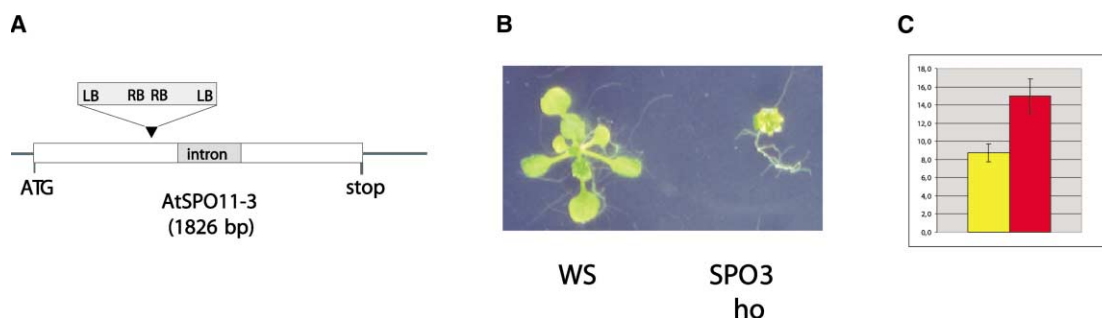


Figure 3. Characterization of the AtSPO11-3 Insertion Mutant of *Arabidopsis*

- (A) Location of the insertion within the gene. The T-DNA insertion is located in exon 1 and is combined with a deletion of 4 bp. The insertion consists of two T-DNAs in an inverse orientation.
- (B) Comparison of a wild-type plant and a plant homozygous for the insertion 2 weeks after germination.
- (C) Statistical analysis of a comet assay. The average values of the percentage of DNA in tails of 7-day-old seedlings of the AtSPO11-3 mutant (red) versus wild-type nuclei WS (yellow). Error bars indicate the standard error values. The medians of 250 comets on 10 individual gels represent 1 experimental point.

for the putative topoisomerase activity. To sustain this hypothesis, we constructed clones in which GFP was fused to the N-terminal 144 or 136 amino acids of AtTop6B and AtSpo11-3, respectively. We analyzed transient GFP expression with a confocal laser scanning microscope after particle bombardment into 2-week-old *Arabidopsis* seedlings. Whereas the GFP protein alone was not targeted to a specific compartment and GFP fused to a chloroplast-targeting signal was targeted to the chloroplasts, the AtSpo11-3 and AtTop6B fusion proteins were targeted to the nucleus (Figure 1G).

To test whether AtTop6B and AtSpo11-3 are parts of a functional entity, we isolated from the Wisconsin library an AtSPO11-3 insertion mutant, which is 440 bp after the start codon, carrying a T-DNA dimer that is in inverse orientation and is integrated in the first exon. Four bp of the original ORF were deleted during T-DNA insertion (Figure 3A). Using RT-PCR, we could not detect mRNA carrying sequences of the gene downstream of the insertion. Thus, at best, the first 146 of 427 amino acids could be expressed. Using PCR, we could demonstrate that plants heterozygous for the insertion grew like wild-type seedlings and plants homozygous for the insertion exhibited a phenotype strikingly similar to the AtTOP6B mutant (Figure 3B). Electron microscopic studies indicated the same structural changes as for the AtTOP6B mutant. Using the comet assay, we detected more DNA breaks (Figure 3C), and via flow cytometry, we detected no nuclei of a polyploidy level of higher than 8C in the mutant (Figure 2C). Via crossing the two heterozygous mutants and consecutive identification by PCR, a double mutant was obtained that showed an identical phenotype as the single mutants; the presence of the identical phenotype demonstrates that both genes act in a common pathway.

Altogether, our results indicate that loss of AtTop6B or AtSpo11-3 function leads to a dramatic reduction of cell proliferation in *Arabidopsis*. Both factors seem to form a functional complex that is involved in DNA replication as well as in endoreduplication in *Arabidopsis*. The phenotype indicates that a certain number of replication cycles can be performed in the mutant background; however, most probably due to the accumulation of unresolved or unspecifically resolved intermediates, cell proliferation and plant development is stopped at a certain stage. It is especially intriguing that the second round of endoreplication (to 8C) is incomplete in the mutant and blocks any further replication. As the archaeobacterial Top VI proteins have topoisomerase II function *in vitro* [5, 6], we assume a similar activity for the complex of AtTop6B and AtSpo11-3. As four type I and one type II topoisomerases [17, 21] can be found in the *Arabidopsis* genome, it remains to be elucidated for which specific aspect of replication and endoreduplication a Top VI function is necessary, a function either not required or taken over by other factors in non-plant eukaryotes. It also remains an open question whether this activity was lost from the common ancestor of yeast and animals after diversion of plants or whether it was gained by plants via horizontal gene transfer from archaeobacteria.

## Experimental Procedures

### Screening and Isolation of the *Arabidopsis* Insertion Mutants

Screening and isolation of the insertion mutants was done as described at the *Arabidopsis* insertion mutant facility (<http://www.biotech.wisc.edu/NewServicesAndResearch/Arabidopsis/>). The AtTOP6B knockout was obtained from the  $\alpha$  population (Vector pD991, kanamycin resistance), and the AtSPO11-3 knockout was obtained from the basta-population (Vector pROK2, phosphinotricin resistance). Both mutants carried only one insertion locus. The background ecotype of the mutants was WS.

### Electron Microscopy

Fixation, substitution, embedding, and electron microscopy analyses of cotyledons was performed as described [22].

### Complementation of the AtTOP6B Mutant

Using the oligonucleotides 5'-dCGAACCCGGGGCTAAGATTC TAGGATTAC-3' and 5'-dCTAGTCTAGACCACITTTCAAGTGTTT GTC-3', a 7.2-kb genomic fragment containing the complete AtTOP6B gene, including 2 kb of the 5' upstream region, was amplified. The fragment was digested with SmaI and XbaI; was cloned in the binary vector pPZP221 [23], harboring the gentamycin resistance gene; and was sequenced. Subsequently, the construct was transformed via *Agrobacterium tumefaciens* (C58) into *Arabidopsis* by using the floral dip method [24].

### GFP Targeting Experiments

Two-week-old seedlings were bombarded with 1  $\mu$ m gold particles at 1100 psi pressure, and the particles were emitted from a PDS-1000/He gun with a Hepta adaptor (BIORAD). The plants were grown on germination medium [15]. One day after bombardment, single leaves of the seedlings were analyzed with the confocal laser scanning system Zeiss LSM 410. Excitation light of 488 nm produced by a krypton/argon laser and a 510–525 nm emission filter allowed detection of GFP-mediated fluorescence.

### Root Culture

The regeneration of calli from root cultures was done as described [15]. The callus-inducing medium contained 0.5 mg/l dichlorophenoxyacetic acid and 0.05 mg/l kinetin. After 4 days, the plant material was transferred to shoot-inducing medium (SIM) containing 5 mg/l 2-isopentenyladenine and 0.15 mg/l indole-3-acetic acid. The calli were transferred every 2 weeks onto new plates.

### Determination of the Mitotic Index

Roots were fixed in ethanol/acetic acid (3/1) and were hydrolyzed in 0.1 N HCl at 60°C for 15 min, squashed in 45% acetic acid, DAPI-stained, and analyzed for mitotic stages with the fluorescence microscope.

### Comet Assay

After embedding nuclei released from razor blade-chopped tissue in agarose on a microscope slide, we lysed the nuclei with sarcosine and 2.5 M NaCl to remove cytoplasm and most nuclear proteins, leaving supercoiled DNA as “nucleoids”. During electrophoresis, broken DNA may migrate to the anode and form a “comet tail” of DNA that extends from the nucleoid. This allows DNA damage to be quantified as a percentage of the DNA in comet tails after propidium iodide staining of DNA under epifluorescence microscope by the Comet module of Lucia software ([www.lim.cz](http://www.lim.cz)). Before electrophoresis in TBE buffer (pH 8.3), short exposure to a pH above that at which DNA denaturation occurs (12.6) allows preferential detection of DNA single-strand breaks [16].

### Flow Cytometry

For preparation of suspensions of nuclei, three plantlets were chopped with a razor blade in 1 ml ice-cold staining buffer in a petri dish; the buffer was supplemented with 50  $\mu$ g/ml propidium iodide (PI) (Molecular Probes) + 50  $\mu$ g/ml DNase-free RNase (Boehringer Ingelheim Bioproducts Partnership) according to a procedure published by Galbraith et al. [25]. The chopped plantlets were then

filtered through a 35  $\mu\text{m}$  mesh (Falcon 12  $\times$  75 mm tube with a 35  $\mu\text{m}$  strainer cap). The analysis was made with a FACStar<sup>PLUS</sup> flow cytometer (Becton Dickinson) equipped with an argon laser INNOVA 90-5 (Coherent) using the analysis program CellQuest. PI fluorescence was excited with 500 mW at 514 nm and was measured in the FL1-channel by using a 630 nm band-pass filter. A total of 10,000 nuclei were measured for each analysis.

#### Acknowledgments

The study was funded by the grant Pu137/6 of the Deutsche Forschungsgemeinschaft. Karel Angelis was supported by Grant Agency of the Czech Republic, project A6038201. We thank the *Arabidopsis* knockout facility of the University of Wisconsin for the *Arabidopsis* seeds, Oliver Berkowitz for the GFP targeting vectors, Bernhard Claus for the CLSM photographs, and Andrea Kunze, Barbara Hildebrandt, Karolina Matesovska, and Jan Adamec for excellent technical assistance.

Received: August 1, 2002

Revised: August 19, 2002

Accepted: August 20, 2002

Published: October 15, 2002

#### References

- Hartung, F., and Puchta, H. (2001). Molecular characterization of homologues of both subunits A (SPO11) and B of the archaeobacterial topoisomerase 6 in plants. *Gene* 271, 81–86.
- Champoux, J.J. (2001). DNA topoisomerases: structure, function, and mechanism. *Annu. Rev. Biochem.* 70, 369–413.
- Wang, J.C. (2002). Cellular roles of DNA topoisomerases: a molecular perspective. *Nat. Rev. Cell Biol.* 3, 430–440.
- Bergerat, A., Gadelle, D., and Forterre, P. (1994). Purification of a DNA topoisomerase II from the hyperthermophilic archaeon *Sulfolobus shibatae*. A thermostable enzyme with both bacterial and eucaryal features. *J. Biol. Chem.* 269, 27663–27669.
- Buhler, C., Gadelle, D., Forterre, P., Wang, J.C., and Bergerat, A. (1998). Reconstitution of DNA topoisomerase VI of the thermophilic archaeon *Sulfolobus shibatae* from subunits separately overexpressed in *Escherichia coli*. *Nucleic Acids Res.* 26, 5157–5162.
- Buhler, C., Lebbink, J.H., Bocs, C., Ladenstein, R., and Forterre, P. (2001). DNA topoisomerase VI generates ATP-dependent double-strand breaks with two-nucleotide overhangs. *J. Biol. Chem.* 276, 37215–37222.
- Nichols, M.D., DeAngelis, K., Keck, J.L., and Berger, J.M. (1999). Structure and function of an archaeal topoisomerase VI subunit with homology to the meiotic recombination factor Spo11. *EMBO J.* 18, 6177–6188.
- Bergerat, A., de Massy, B., Gadelle, D., Varoutas, P.C., Nicolas, A., and Forterre, P. (1997). An atypical topoisomerase II from Archaea with implications for meiotic recombination. *Nature* 386, 414–417.
- Keeney, S., Giroux, C.N., and Kleckner, N. (1997). Meiosis-specific DNA double-strand breaks are catalyzed by Spo11, a member of a widely conserved protein family. *Cell* 88, 375–384.
- Keeney, S. (2001). Mechanism and control of meiotic recombination initiation. *Curr. Top. Dev. Biol.* 52, 1–53.
- Villeneuve, A.M., and Hillers, K.J. (2001). Whence meiosis? *Cell* 106, 647–650.
- Hartung, F., and Puchta, H. (2000). Molecular characterization of two paralogous SPO11 homologues in *Arabidopsis thaliana*. *Nucleic Acids Res.* 28, 1548–1554.
- Grelon, M., Vezon, D., Gendrot, G., and Pelletier, G. (2001). AtSPO11-1 is necessary for efficient meiotic recombination in plants. *EMBO J.* 20, 589–600.
- Krysan, P.J., Young, J.K., and Sussman, M.R. (1999). T-DNA as an insertional mutagen in *Arabidopsis*. *Plant Cell* 11, 2283–2290.
- Valvekens, D., van Lisjebettens, M., and van Montagu, M. (1992). *Arabidopsis* regeneration and transformation (Root explant system). In *Plant Tissue Culture Manual A8*, K. Lindsey, ed. (Netherlands: Kluwer Academic Publishers), pp. 1–17.
- Angelis, K.J., Dušinská, M., and Collins, A.R. (1999). Single cell gel electrophoresis: detection of DNA damage at different levels of sensitivity. *Electrophoresis* 20, 2133–2138.
- The Arabidopsis Genome Initiative. (2000). Analysis of the genome sequence of the flowering plant *Arabidopsis thaliana*. *Nature* 408, 796–815.
- Garcia, V., Salanoubat, M., Choisne, N., and Tissier, A. (2000). An ATM homologue from *Arabidopsis thaliana*: complete genomic organisation and expression analysis. *Nucleic Acids Res.* 28, 1692–1699.
- Larkins, B.A., Dilkes, B.P., Dante, R.A., Coelho, C.M., Woo, Y.M., and Liu, Y. (2001). Investigating the hows and whys of DNA endoreduplication. *J. Exp. Bot.* 355, 183–192.
- Joubes, J., and Chevalier, C. (2000). Endoreduplication in higher plants. *Plant Mol. Biol.* 43, 735–745.
- Xie, S., and Lam, E. (1994). Abundance of nuclear DNA topoisomerase II is correlated with proliferation in *Arabidopsis thaliana*. *Nucleic Acids Res.* 22, 5729–5736.
- Börnke, F., Hajirezaei, M., Heineke, D., Melzer, M., Herbers, K., and Sonnewald, U. (2002). High level production of the non-cariogenic sucrose isomer palatinose in transgenic tobacco plants strongly impairs development. *Planta* 214, 356–364.
- Haidukiewicz, P., Svab, Z., and Maliga, P. (1994). The small, versatile pPZP family of *Agrobacterium* binary vectors for plant transformation. *Plant Mol. Biol.* 25, 989–994.
- Clough, S.J., and Bent, A.F. (1998). Floral dip: a simplified method for *Agrobacterium*-mediated transformation of *Arabidopsis thaliana*. *Plant J.* 16, 735–743.
- Galbraith, D.W., Harkins, K.R., Maddox, J.M., Ayres, N.M., Sharma, D.P., and Firoozabady, E. (1983). Rapid flow cytometric analysis of the cell cycle in intact plant tissues. *Science* 220, 1049–1051.